A high-Q Tunable Grounded Negative Inductor for Small Antennas and Broadband Metamaterials

Emilie Avignon-Meseldzija, Pietro Maris Ferreira, Lekkas Konstantinos,
Fabrice Boust

A high-Q Tunable Grounded Negative Inductor for Small Antennas and Broadband Metamaterials

Emilie Avignon-Meseldzija[1], Pietro Maris Ferreira[1], Konstantinos Lekkas[2], Fabrice Boust[2,3]

{emilie.avignon, pietro.maris, konstantinos.lekkas, fabrice.boust}@centralesupelec.fr

[1]GeePs, UMR CNRS 8507, Department of Mixed Signal Circuits and Systems, CentraleSupélec, Gif-Sur-Yvette, France
[2]SONDRA Laboratory, CentraleSupélec, Gif-Sur-Yvette, France
[3]Department of Electromagnetism and Radar, ONERA – The French Aerospace Lab, Palaiseau, France

Abstract—**This paper presents a broadband high-Q tunable negative inductor based on a gyrator topology. In order to reduce the risk of instability and to increase circuit bandwidth, simple inverters are used as transconductance amplifier. A complete stability analysis and careful circuit design details using SOI 180 nm technology are presented. Post-layout simulations results show a negative inductance variation from -24 nH to -13.7 nH. For a bandwidth from 10 MHz to 1 GHz, inductance value error remains under 12.5 %. Circuit power consumption is 16 mW; and area consumption is 120 μm by 84 μm.**

Keywords—gyrator; stability analysis; non-Foster circuits; negative inductance;

I. INTRODUCTION

Since 1999, when the first metamaterial was proposed by Pendry et al. [1], there is a tremendous interest by the research community for metamaterials and their applications (antenna miniaturization, invisibility cloaks, sub-wavelength imaging etc). Metamaterials such as rod mediums and split ring resonators allow the synthesis of negative permittivity and negative permeability respectively [1]. However, these characteristics present a narrowband behavior due to the inherent limitations of passive metamaterials [2,3]. In order to increase their limited bandwidth, the use of negative capacitors and negative inductors has been proposed in [4-6].

These negative devices are named are non-Foster circuits because they violate Foster's Theorem. According to Foster [7], the reactance of any passive device should increase monotonically with the frequency. Broadband non-foster circuits embedded in a metasurface [8,9] are very promising in the design of broadband patch-antennas or cloaks. Additionally, the capability of non-Foster circuits to increase the bandwidth of electrically small antennas (possibly combined with metamaterial) has already been demonstrated in [10-12].

Some topologies, as Linvill [13] or gyrator [14], have been proposed in the literature to design negative capacitors and negative inductors. Compared to Linvill OCS, gyrator topology achieves a higher quality factor (Q). Nevertheless, Linvill OCS may reach high-Q at the expense of power consumption [18]. In a high-Q gyrator topology, positive active inductors are stable [14], however negative inductors are often unstable. Thus, the main challenge is guaranteeing the stability condition in a high-Q circuit.

In this paper, a broadband high-Q tunable negative inductor is proposed using SOI 180 nm. A gyrator topology is chosen because it is possible to tune negative-inductance value through a varactor. The rest of this paper is organized as follows. Section II defines stability condition in gyrator-based negative inductors regarding the load. Section III presents the circuit architecture and its dimensioning. Section IV presents post-layout simulation, verifies stability conditions defined in Section II and provides a comparison of this work with recent published works on negative inductances. Finally, conclusions are presented.

II. STABILITY ANALYSIS

A. Stability issue for single negative inductor

Gyrator-based active inductors are designed using two back-to-back transconductors and a capacitor. Although positive active inductors use a positive and a negative transconductor, negative inductors use two transconductances with the same sign. The circuit topology of a gyrator-based negative inductor is presented in Fig. 1 considering parasitic devices.
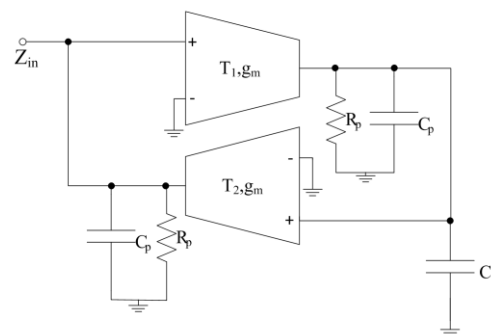

Fig. 1. The gyrator topology, with a capacitive load for the synthesis of a negative inductor

In Fig. 1, C_p and R_p are the total parasitic capacitances and resistances at the output and input of the transconductances. To synthesize a negative inductor, the gyrator load (C) should be capacitive. Thus, the circuit shown in Fig. 1 is equivalent to

the model presented in Fig. 2. For this model, the expression of the input impedance is:

$$Z_{in}(s) = \frac{R_p R_{neg} + R_p L_{neg} s}{C_p R_p L_{neg} s^2 + (C_p R_p R_{neg} + L_{neg})s + R_{neg} + R_p} \quad (1)$$

where

$$L_{neg} = -\frac{C_p + C}{g_m^2} \quad (2)$$

and

$$R_{neg} = -\frac{1}{g_m^2 R_p} \quad (3)$$

For stability analysis of the negative inductors, pole analysis in input impedance modelling (see Eq. (1)) is considered. From the expression of the poles, two cases can be distinguished:

1) When $R_p > R_{neg}$: which is the case to obtain a high Q. The input impedance of the circuit is resistive up to ω_z given by (4) then inductive between ω_z and ω_0 given by (5), and capacitive after ω_0 [14]. It should be emphasized that under this condition, one of the poles has a positive real part and hence the negative inductor alone is unstable.

$$\omega_z = \frac{R_{neg}}{L_{neg}} \quad (4)$$

$$\omega_0 = \sqrt{\frac{R_p + R_{neg}}{R_p C_p L_{neg}}} \quad (5)$$

2) When $R_p < R_{neg}$: both poles obtained from Equation (1) have a negative real part and the system is stable. However, in this case the impedance of the circuit is mainly resistive or capacitive but not inductive anymore. Moreover, it will be useless to place it in shunt with a small antenna or metamaterial, because it will not compensate an inductive characteristic.
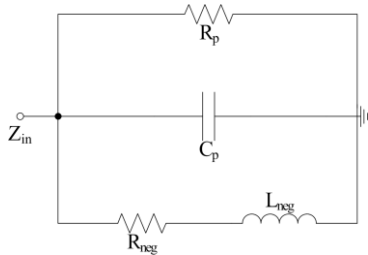
Fig. 2. The equivalent circuit of the gyrator

In an appropriate manner, it is mandatory to verify the stability of the association of the high-Q gyrator-based negative inductance and the structure to be compensated.

B. Stability of the system

Chosen approach is to take into account a model standing either for a metamaterial or an antenna and insure that it will be stable in parallel with the proposed gyrator-based high-Q negative inductor. This model is composed of a positive resistor R_{pos} in series with a positive inductance L_{pos}. To check the stability of the whole system, the poles of the gyrator-based high-Q negative inductance in parallel with the model are considered. These poles must have a negative real part.

Fig. 3 presents the roots-locus obtained for the negative inductor modelling with the following parameters: L_{neg} = -10 nH, R_{neg} = -12 Ω, C_p = 0.3 pF, and R_p = 2 kΩ. Concerning the model of metamaterial or antenna in parallel, two cases are considered. In Fig. 3a, metamaterial or antenna modelling considers R_{pos} = 0 Ω when increasing L_{pos} from 2 nH to 10 nH. In Fig. 3b, metamaterial or antenna modelling considers L_{pos} = 5 nH and R_{pos} varying from 1 to 12 Ω. The stability analysis conclusions are:

(a) for a pure positive inductor, the system is stable for values about two times lower than the absolute value of the negative inductor (Fig. 3a).

(b) for a positive inductor satisfying this condition, the series resistor has to remain under the absolute value of R_{neg} (Fig. 3b).

Finally simplified conditions to keep stability are:

$$\begin{cases} L_{pos} \leq \dfrac{|L_{neg}|}{2} \\ R_{pos} < |R_{neg}| \end{cases} \quad (6)$$

These stability conditions will be validated in Section IV by a stability analysis using a transient simulation.
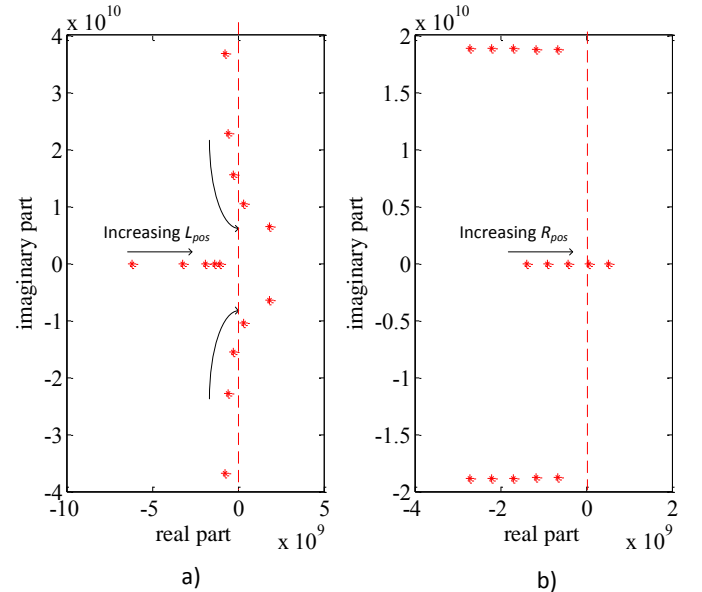
Fig. 3. Root locus a) Rpos = 0 and increasing values of Lpos b) Lpos = 5 nH and increasing values of Rpos

III. GYRATOR-BASED NEGATIVE INDUCTOR

Fig. 4 illustrates the proposed gyrator-based negative inductor in parallel with an antenna or metamaterial model. The circuit supply voltage is V_{DD}=1.65 V and V_{SS} = -1.65 V. Transconductance amplifiers are simple inverters which have an advantage of no intrinsic poles which potentially lead to instability [15] or bandwidth reduction. Other advantages of

such transconductance amplifier are the reduced complexity and high output impedance, leading to a higher Q.

The drawback is an unavoidable offset between stages, which is removed with a high-pass filter. To keep the advantage of high output impedance, resistances of high-pass filters have been chosen with a large value (50 kΩ). Such high values of resistances are available in SOI 180 nm design kit by high-Ohmic sheet resistors. Capacitances of high-pass filters have been chosen to achieve a cut-off frequency of 3.5 MHz.

To reduce parasitic capacitances of transconductance amplifiers, isolated transistors are chosen to inverter implementation. Aiming an L_{neg} from -20 nH to -10 nH, transconductance amplifiers are designed considering the compromise between g_m and C_p (mostly due to transistor's C_{GS}). It is found a g_m=7.4 mS, and C_p=600 fF. Transistor sizing is presented in Fig. 4.

The tunability of gyrator-based negative inductor is achieved through a varactor. Designed varactor is composed by a couple of PMOS transistors with a drain-source connection, and the bulk connected to V_{DD} [16]. The tunable range required to the varactor is from 100 fF to 800 fF.
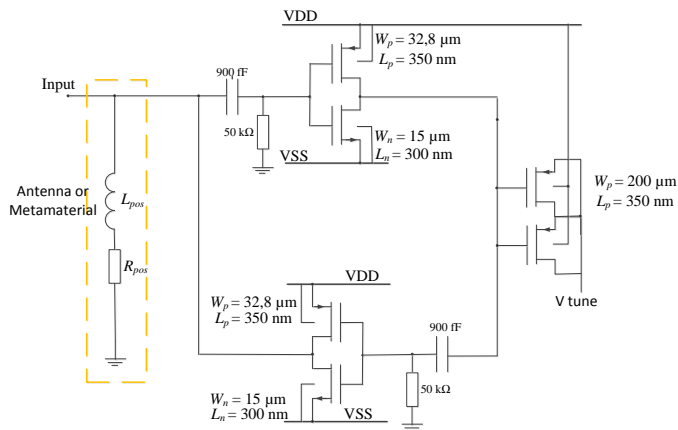
Fig. 4. Transistor level schematic of the circuit

IV. POST-LAYOUT SIMULATION RESULTS

Circuit layout is presented in Fig. 5, having 120 μm by 84 μm of area. A large area is dedicated to the varactor. Ground plane is omitted in Fig. 5 for an improved clearness. Post-layout simulation results are presented in Fig. 6. Input impedance real and imaginary parts are obtained for boundary V_{tune} values of 0 V and 1 V. Negative inductance variation is demonstrated from -24 nH to 13.7 nH with an error smaller than 12.5% in broadband from 10 MHz to 1 GHz. Post-layout simulations reveals a Q greater than 5. Power consumption is evaluated to 16 mW.

To check circuit stability in parallel with metamaterial or antenna model, a transient post-layout simulation is performed. This stability analysis is able to detect hidden modes which leads to circuit instability. Thus, a narrow current pulse of 1 mA has been injected at each node of the circuit of the circuit. The width of the pulse has been chosen

equal to 0.1 ns in order to cover a large spectrum and trigger oscillation if the system is unstable.
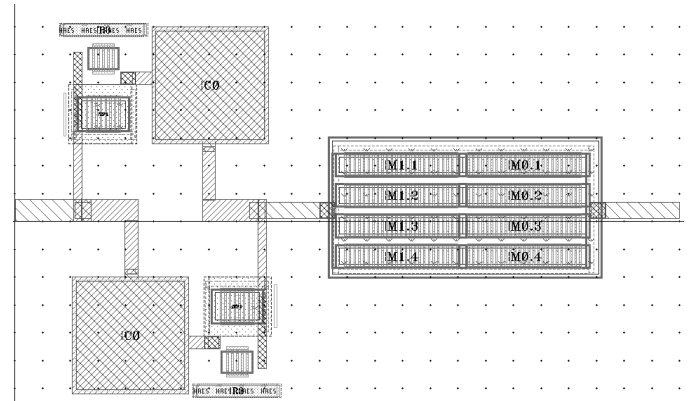
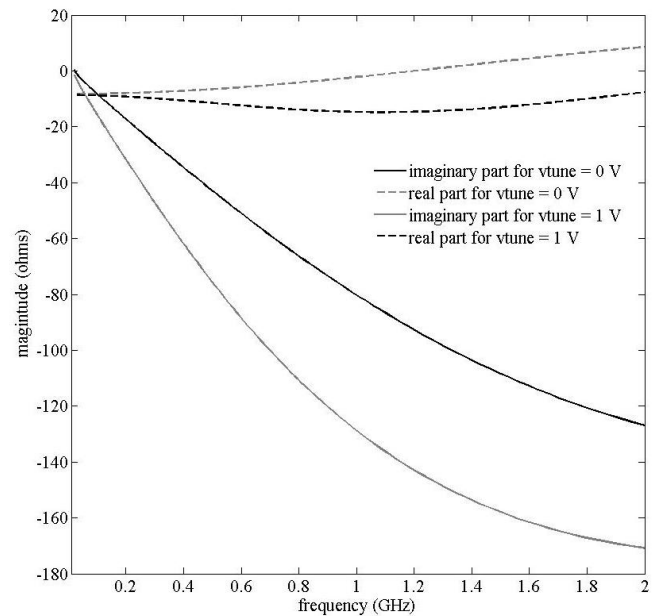Fig. 5. Layout view (ground plane omitted for clarity reasons)

Fig. 6. Imaginary and real part of the input impedance of the IC layout for different values of Vtune

No instability was detected, as conditions presented in Eq. (6) were fulfilled. Fig. 7 presents the input voltage obtained after the injection of the current pulse for two models:

(a) when L_{pos} = 5 nH and R_{pos} = 10 Ω, oscillations are found due to $R_{pos} > |R_{neg}| = 6\ \Omega$

(b) when L_{pos} = 5 nH and R_{pos} = 5 Ω, system is stable as $R_{pos} < |R_{neg}|$.

Performance degradation due to process variability is estimated using 200 point Monte Carlo simulation at 500 MHz. For V_{tune} =0 V, circuit has μ_Q=5.88 and σ_Q = 0.78, μ_{Lneg}=-13.66 nH and σ_{Lneg} = 0.45 nH. For V_{tune} =1 V, circuit has μ_Q=5.96 and σ_Q = 0.48, μ_{Lneg}=-24.33 nH and σ_{Lneg} = 0.68 nH.
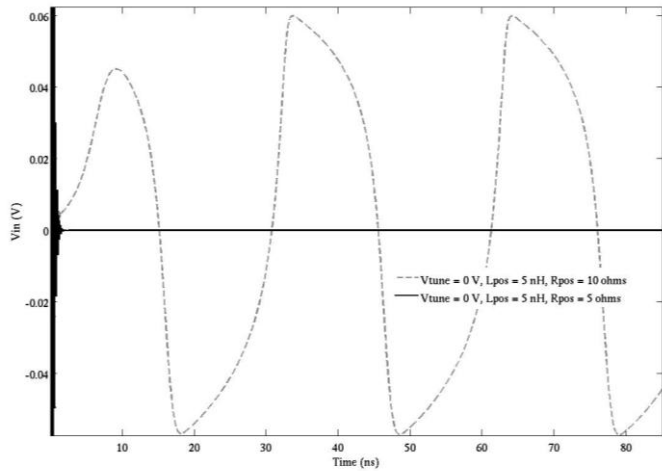
Fig. 7. Input voltage when applying a current pulse for Vtune = 0 V and Vtune = 1 V

Table 1 presents a comparison of post-layout simulations of the proposed circuit and measurement results of state-of-the-art circuits. In [17-19], Q is not often presented, thus Q has been evaluated by the ratio between imaginary and real parts.

Table 1. State-of-the-art comparison

Ref.	Method	BW (GHz)	Q	Technology	Power consumption
This work	Single Gyrator (grounded)	0.01-1	> 5	SOI 180 nm	16 mW
[17]	Differential Gyrator (floating)	0.01-1	> 5	8HP BiCMOS	35 mW
[18]	Linvill's OCS (floating)	0.1-6	< 1	65 nm bulk CMOS	5 mW
[19]	Linvill's SCS (grounded)	0.001-0.5	< 1	CMOS 0.5 µm	33 mW

V.   CONCLUSION

A broadband high-Q tunable negative inductor has been proposed to compensate a positive inductive part in small antennas or broadband metamaterials increasing their bandwidth. A gyrator-based topology using simple inverters was chosen in order to create a tunable negative inductor with high Q, reduced complexity, and low power consumption. Moreover, the use of inverter for transconductance amplifiers reduces the risk of instability and increases circuit bandwidth.

Pos-layout simulations have been presented. Negative inductor is tunable from -24 nH to -13.7 nH; having maximum error under 12.5 % up to 1 GHz bandwidth. Circuit power consumption is 16 mW; and area consumption is 120 µm by 84 µm.

REFERENCES

[1] J. B. Pendry, A. J. Holden, D. J. Robbins, W. J. Stewart, "Magnetism from Conductors and Enhanced Nonlinear Phenomena", *IEEE Transactions on Microwave Theory and Techniques*, vol. 47, no.11, pp.2075-2084, Nov. 1999.

[2] S. Tretyakov, S. Maslovski, "Veselago Materials: What is possible and impossible about the dispersion of the constitutive parameters", *IEEE Antennas and Propagation Magazine*, vol. 49, no. 1, pp. 37-43, Feb 2007

[3] S. Tretyakov, S. Maslovski, A. Sochava, C. Simovski, "The influence of Complex Material Coverings on the Quality Factor of Simple Radiating Systems", *IEEE Transactions on Antennas and Propagation*, vol. 53, no.3, pp. 965-970, Mar. 2005.

[4] S. Hrabar, I. Krois, and A. Kiricenko, "Towards active dispersionless ENZ metamaterial for cloaking applications", *Metamaterials*, vol. 4, pp.89-97, 2010.

[5] W. Xu, W. J. Padilla, and S. Sonkusale, "Loss compensation in Metamaterials through embedding of active transistor based negative differential resistance circuits", *Optics Express*, vol. 20, pp. 22406-22411, 2012.

[6] S. Hrabar, I. Krois, I. Bonic, and A. Kiricenko, "Negative capacitor paves the way to ultra-broadband metamaterials", *Applied Physics Letters*, vol. 99, pp. 254103, 2011.

[7] R. M. Foster, "A reactance theorem", *Bell Syst. Tech. J.*, vol. 3, pp. 259–267, 1924.

[8] P. Y. Chen, C. Argyropoulos, and A. Alù, "Broadening the Cloaking Bandwidth with Non-Foster Metasurfaces", *Physical Review Letters*, vol. 111, p. 233001, 2013.

[9] S. Saadat, M. Adnan, H. Mosallaei, E. Afshari, "Composite Metamaterial and Metasurface Integrated With Non-Foster Active Circuit Elements: A Bandwidth-Enhancement Investigation", *IEEE Transactions on Antennas and Propagation*, vol 61, no. 3, pp. 1210-1218, Mar. 2013.

[10] K. Perry, "Broadband antenna systems realized from active circuit conjugate impedance matching", *MS Thesis*, Naval Postgraduate School, Monterey, 1973

[11] S. E. Sussman-Fort and R. M. Rudish, "Non-Foster impedance matching of electrically-small antennas", *IEEE Transactions on Antennas and Propagation*, vol. 57, pp. 2230-2241, 2009.

[12] N. Zhu and R. W. Ziolkowski, "Design and measurements of an electrically small, broad bandwidth, non-Foster circuit-augmented protractor antenna", *Applied Physics Letters*, vol. 101, pp. 024107, 2012.

[13] J. G. Linvill, "Transistor negative impedance converters", *Proc IRE*, vol. 41, pp. 725-729, Jun. 1953

[14] F. Yuan, "CMOS Active Inductors and Transformers: Principle, Implementation and Applications", Springer, 2008

[15] B. Nauta, "Analog CMOS Filters for Very High Frequencies", Kluwer Academic Publishers, 1993.

[16] Ryan Leee Bunch, Sanjay Raman, "Large-Signal Analysis of MOS varactors in CMOS-Gm LC VCOs" *IEEE Journal of Solid-State Circuits*, Vol. 38, No. 8, Aug. 2003.

[17] Carson R. White, Jason W. May, Joseph S. Colburn "A Variable Negative-Inductance Integrated Circuit at UHF Frequencies", *IEEE Microwave and Wireless Components Letters*, Vol. 22, No. 1, Jan. 2012.

[18] Soheil Saadat, Hamidreza Aghasi, Ehsan Afshari, Hossein Mosallei "Low-Power Negative Inductance Integrated Circuits for GHz Applications", *IEEE Microwave and Wireless Components Letters*, vol. 25, No. 2, Jan. 2015.

[19] John M. C. Covington III, Kathryn L. Smith, Joshua W. Shehan, Varun S. Kshatri "Measurement of a CMOS Negative Inductor for Wideband Non-Foster Metamaterials", *IEEE SoutheastCon*, Lexington Mar. 13-16th 2014.